

Agroforestry Land Use Land Cover Area Classification Using Decision Tree Algorithm

Arief Darmawan, Trio Santoso*, Rudi Hilmanto

Department of Forestry, Faculty of Agriculture, Universitas Lampung, Jl. Prof. Dr. Sumantri Brojonegoro 1, Bandar Lampung, Indonesia 35145

Received January 10, 2024/Accepted December 4, 2024

Abstract

Monitoring the location and extent of agroforestry land use land cover (LULC) in Lampung Province is critical for effective policy development and sustainable agroforestry management. However, existing monitoring efforts have been limited to small regions. This study addressed this gap by employing threshold values from five distinct vegetation indices (ARVI, EVI, GDVI, NDVI, and SAVI) derived from Landsat 9 OLI imagery to accurately identify and estimate agroforestry LULC across the Lampung Province. The data collection activities were carried out using a combination of Landsat 9 OLI satellite imagery acquisition, and ground truth validation on 7 classes of different land use (forest, agroforestry, dry land farming, ricefield, settlements, bare land, and water bodies) within 5,600 points of interest (POI) inside 5 regencies as an area of interest (AOI). This study aimed to predict agroforestry area based on vegetation indices (VIs) threshold using the decision tree (DT) algorithm. The research process involved a series of systematic steps, beginning with satellite image data acquisition and preprocessing, VIs values extraction, and DT sequential for agroforestry areas. The DT computation incorporated the value of each LULC type on the 5 VIs. The result showed that the overall accuracy reached 91.59% with a Kappa coefficient of 0.89, indicating a high level of accuracy for land cover identification. The DT algorithm calculation showed that the agroforestry in Lampung Province estimated spanned for 734,739.61 ha, determined only by NDVI and ARVI. The findings have significant implications for both policy development and agroforestry management. Accurate LULC classification enhances decision-making processes by providing reliable data on land use patterns, which can guide sustainable land management practices and support the creation of region-specific agroforestry policies. This research directly informs policymakers on the extent and distribution of agroforestry areas, offering a foundation for crafting strategies aimed at promoting sustainable land use while mitigating environmental degradation. The methodology also provides a scalable approach for other regions facing similar agroforestry and land management challenges.

Keywords: agroforestry, Lampung Province, Landsat 9 imagery, vegetation index, decision tree algorithm

*Correspondence author, email: trio.santoso1003@fp.unila.ac.id

Introduction

Agroforestry systems, which integrate commercial plant cultivation with forestry components such as trees, were employed by the local communities in Lampung Province to address their economic and environmental needs. These systems have been established by combining various tree crops, many of which are food-producing plants, to create a diverse and sustainable land-use approach (Santoso et al., 2023). These systems also encompass livestock farming, plantations, fisheries, and beekeeping. To manage these activities concurrently, adapted planting patterns were implemented by the preferences of the farmers and the characteristics of the landscape (Alhabsyi et al., 2020; Narendra et al., 2021; Santoso et al., 2021; Saufi & Saleh, 2021; Visnhu, 2021; Harianto et al., 2022).

Agroforestry was selected as the mitigation strategy due to its established efficacy in addressing land use changes and constraints, thereby preventing the detrimental effects of environmental degradation, including pollution, erosion, flooding, and landslides (Aryal et al. 2018; Gama-Rodrigues et al. 2021; Gosling et al. 2020; Octavia et al. 2022).

The advantages encompass farmers to produce a diverse range of commodities and having the ability to plan harvests

at different intervals and the capacity to plan harvests at various intervals, potentially generating a consistent and sustainable income throughout the year (Jezeer et al., 2019; Tschora & Cherubini, 2020; Warren-Thomas et al., 2020). This stands in opposition to monoculture land management, in which producers are remunerated solely following the harvest season.

Agroforestry practices implemented in Lampung Province involve the cultivation of fruit-bearing trees such as pinang (*Areca catechu* L.), petai (*Parkia speciosa* Hassk.), jengkol (*Pithecellobium lobatum* Benth.), coffee (*Coffea robusta* L. Linden), and cocoa (*Theobroma cacao* L.), which are regarded as high-value plantation crops. Additionally, nutmeg (*Myristica fragrans* Houtt.) and other varieties with high economic value are incorporated as alternative families into the plantation practices (Wanderi et al., 2019; Prasetya et al., 2020; Afifah et al., 2021; Harianto et al., 2022).

The significance of the advantages associated with agroforestry must be substantiated by data-driven planning that is promptly and precisely executed so that it may serve as the foundation for establishing sustainable policies that are effective. Hence, the monitoring of agroforestry land extent and distribution is an urgent matter, as current monitoring

efforts in the Lampung Province region are confined to a small area and rely on recognition methods that combine channels (bands) and pixel values. Consequently, the image exhibits numerous deficiencies in object recognition, which can be attributed to the province's enormous size and the prevalence of clumsy vegetation.

An alternative approach involves the integration of threshold values from multiple vegetation indices (Vis), which are numerical values derived from remote satellite image data and serve as indicators of the extent of green vegetation within a given region, in order to classify agroforestry land use land cover (LULC) categories (Rahma, 2020; Sari et al., 2022). VI is calculated using reflectance values of different wavelengths of light, such as red and near-infrared, which are sensitive to the chlorophyll content of vegetation (Huang & Lian, 2015; Jorge et al., 2019; Guerini Filho et al., 2020; Setiawan et al., 2021; Ardiansyah et al., 2022). There are various types of VIs, each with its own specific algorithms and applications (Zhao et al., 2018; Gao et al., 2020; Pôças et al., 2020). Some popular types of VIs include normalized difference vegetation index (NDVI) and enhanced vegetation index (EVI) (Miller et al., 2019; Binte Mostafiz et al., 2021; Huang et al., 2021; Li et al., 2021; Roy,

2021; Xie & Fan, 2021).

Landsat 9 OLI has been widely used for monitoring research and land cover changes in Indonesia (Antomi, 2022). Including monitoring of changes in LULC research (Salma et al., 2022). This was feasible due to the accessibility and simplicity with which individuals can acquire data from images encompassing diverse resolutions and image bands (Benharrats & Mahi, 2020).

Landsat image data can be utilized as a basis imagery for the computation of VIs for LULC identification (Setiawan et al., 2013; Sholihah et al., 2016; Hidayati et al., 2019; Oon et al., 2019). Despite the fact that Landsat 9 imagery, which possesses the identical wavelength range as Landsat 8, has not been extensively employed in similar studies, this presents an opportunity to evaluate its efficacy in the present research. In light of this circumstance, land use identification research utilizing Landsat 9 imagery as a foundation for computing the vegetation index must be undertaken.

Methods

Study area The study was conducted within the Lampung Province area (Figure 1) that was located between latitude S3°45'00" to S4°5'00" and longitude E103°48'00" to

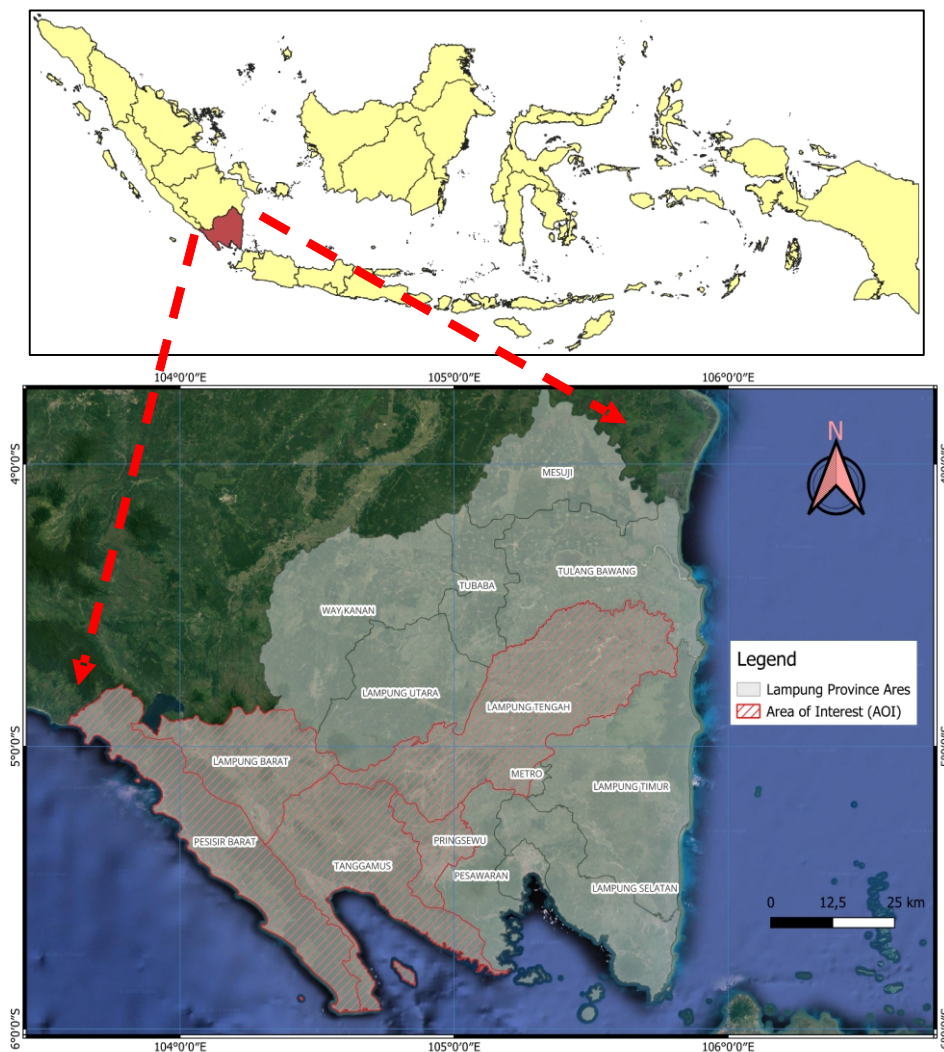


Figure 1 Research location.

E105°45'00" (Romli et al., 2019). The area of Lampung was 33,575.41 km² with 15 regencies. The population of Lampung Province censused in 2022 reached 9,176,600 inhabitants, with a population density 273 km⁻² with population growth of 1.07% and a gender ratio of 104.86 which means the proportion of men is higher than women. The Lampung Province has varied geomorphological landscapes, from hilly and mountainous to coastal and river basins (BPS Provinsi Lampung, 2023).

Landsat datasets The Landsat 9 OLI satellite imagery data utilized in this study were acquired from the official website of the United States Geographical Survey Agency (USGS), which provides open access data via link address <https://earthexplorer.usgs.gov>. Landsat 9 was launched on 11 February 2013 and carries two scientific instruments: the Operational Land Imager (OLI) (Markham et al. 2016; Masek et al. 2020). The two sensors offer comprehensive coverage of the Earth's terrestrial surface throughout the year. They capture data at a high level of detail, with a spatial resolution of 30 m for visible, near-infrared, and shortwave infrared wavelengths, 100 m for thermal, and 15 m for panchromatic images (Table 1) (Wu et al., 2019). The Landsat 9 OLI data was selected to encompass the portion of Lampung Province (Path and Row 123 and 63, 123 and 64, 124 and 63, 124 and 64) with maximum land cloud cover of 10% as the minimum criteria between February and April 2023. To minimize the effect of clouds and haze, we selected Landsat 9 imagery carefully from January to May 2023.

Ground truth validation of land use types Validation of land use types in this research was done by carefully selecting five regencies as the area of interest (AOI), which can represent the overall condition of Lampung Province land use. AOI were designated areas where testing for land use or LULC is done (Logsdon et al., 1996; Rwanga & Ndambuki, 2017; Li et al., 2021).

Land use types of the study area were classified into seven categories, namely: forest, agroforestry, dry land farming, ricefield, settlements, bare land, and water bodies. Where forest areas were determined based on the forest land cover map issued by the Ministry of Environment and Forestry of Indonesia (MoEF, 2021).

The five regency areas in Lampung Province that were selected as AOIs in this study namely: Bandar Lampung

(AOI 1), Pringsewu (AOI 2), Lampung Tengah (AOI 3), Lampung Barat (AOI 4), and Pesisir Barat (AOI 5).

The selection of specific AOIs was strategically done to ensure that the chosen regions accurately represented the diverse land use and land cover types across Lampung Province. Each AOI was selected based on its unique environmental and agricultural characteristics, which are essential for developing a robust and comprehensive classification model. Although the study aimed to classify the entire province, focusing on these AOIs allowed for more detailed and precise ground truth validation and calibration of the decision tree (DT) algorithm.

The selected AOIs encompass critical land use categories, such as forest, agroforestry, dry land farming, rice fields, settlements, and water bodies. These areas were chosen to cover the full spectrum of agroforestry practices and other land cover types present in the region, enabling a balanced and comprehensive dataset for the model. Moreover, these AOIs were diverse enough to capture the heterogeneity in land cover across Lampung, ensuring that the classification results could be generalized across the entire province.

By combining the classification of the whole province with the specific focus on these AOIs for validation, we were able to achieve both detailed accuracy and broader regional applicability, which strengthens the reliability of the classification and its implications for policy and land management.

Numerous communities could be best represented by AOI 1, while AOI 3, AOI 4, and AOI 5 all contain sizable tracts of forest. In Lampung Tengah Regency, there were lots of rice fields, open spaces, water bodies, and dry land agriculture. In the AOI 2, AOI 3, AOI 4, and AOI 5, agroforestry is extensively practiced.

To determine the sampling points used to verify the digital value of the vegetation index, the point of interest (POI) of the seven types of LULC was determined using the fishnet method (Santoso et al., 2021). The fishnet approach was used due to its inherent processing benefits, efficiency, and ease in analysis (Xu et al., 2017; Musiaka & Nalej, 2021). POI was a specific location that researchers found interesting for conducting research. POIs carefully selected and verified repeatedly through field surveying and recorded via GPS (Damayanti et al. 2017; Akmal et al. 2021; Maponya et al. 2021). The number of POIs for a single type of land use

Table 1 Technical description of spatial and spectral resolution of Landsat 9 OLI/TIRS image

Bands	Wavelength (µm)	Resolution (mm)
Band 1 - Visible coastal aerosol	0.43–0.45	30
Band 2 - Visible blue	0.45–0.51	30
Band 3 - Visible gGreen	0.53–0.59	30
Band 4 - Red	0.64–0.67	30
Band 5 - Near infrared (NIR)	0.85–0.88	30
Band 6 - SWIR 1	1.57–1.65	30
Band 7 - SWIR 2	2.11–2.29	30
Band 8 - Panchromatic	0.50–0.68	15
Band 9 - Cirrus	1.36–1.38	30
Band 10 - Thermal infrared (TIRS) 1	10.60–11.19	100
Band 11 - Thermal infrared (TIRS) 2	11.50–12.51	100

per AOI is 160, resulting in a total of 1,120 POIs for each AOI and a total of 5,600 POIs for all AOIs (AOI 1 AOI 5).

The 5,600 POIs were distributed across the five AOIs, which were selected to represent diverse LULC types in Lampung Province. The number of sample points follows the principle of remote sensing research, which states that the number of samples in land use classification is determined based on the number of pixels that can represent each LULC type, ranging from 10 N to 100 N, where N is the number of LULC types (Dogru et al., 2020). The POIs were divided into separate training sets (70%) and testing sets (30%). Specifically, a portion of the POIs was used to train the DT model, while the remaining data was reserved for testing and validating the classification results. This separation ensures that the model was not tested on the same data it was trained on, thereby providing a more realistic assessment of its accuracy.

LULC validation Validating the land use classification was a prerequisite for confirming temporal land use changes (van Vliet et al., 2016; Tsendbazar et al., 2021). The evaluation was conducted using an error matrix, which provided overall accuracy and K coefficient values for each valid land use (Shishir & Tsuyuzaki, 2018). The confusion matrix provides a comprehensive assessment of the accuracy of individual object classifications as well as the overall interpretation (Pahleviannur, 2019). Accuracy calculations are performed by comparing the number of matches between sample point calculations derived from image interpretation data and the actual conditions observed in the field. A confusion matrix integrates calculations from multiple formulas, namely: user's accuracy, procedure's accuracy, and overall accuracy.

User accuracy provides the classification outcomes for each category in which the user has participated. The LULC classes POIs that are represented during classification were represented in the accuracy method. Overall accuracy refers to the proportion of correctly classified instances out of the total number of observations. It is calculated by dividing the sum of correctly classified observations (the diagonal values in the confusion matrix) by the total number of observations, as shown in the formula provided. User's accuracy, procedure's accuracy, and overall accuracy were calculated as shown in Equation [1], Equation [2], and Equation [3] (Berhane et al., 2018; Maxwell et al., 2021; Mishra et al., 2021).

$$\text{User's accuracy} = \frac{X_{ii}}{X_{+i}} \times 100\% \quad [1]$$

$$\text{Prosedur's accuracy} = \frac{X_{ii}}{X_{i+}} \times 100\% \quad [2]$$

$$\text{Overall accuracy} = \frac{\sum_i^r X_{ii}}{N} \times 100\% \quad [3]$$

note: X_{ii} , X_{+i} , X_{i+} , and N consist of the diagonal value of the contingency matrix i -row i -column, the number of types in row i , the number of types in column i , and the number of all observation points, respectively.

The degree of accuracy of the points of interest utilized in the study determined using the Kappa coefficient was also

computed. Since overall accuracy was typically seen to be overestimated, it was currently advised to examine the Kappa coefficient value (Jaya & Etyarsah, 2021). The overall accuracy number only includes correct data between classification results and field circumstances; in contrast, the Kappa coefficient accounts for the error factor in the classification process, resulting in a lower Kappa index value. The Equation [4] is the formula for computing the Kappa coefficient mathematically (Rwanga & Ndambuki, 2017),

$$K = \frac{\sum_{i=1}^1 \pi_{ii} - \sum_{i=1}^1 \pi_{i+} \pi_{+i}}{1 - \sum_{i=1}^1 \pi_{i+} \pi_{+i}} \quad [4]$$

note: K is the Kappa value, $\sum_{i=1}^1 \pi_{ii}$ is the total diagonal proportion of observation frequencies, $\sum_{i=1}^1 \pi_{i+} + \pi_{+i}$ is the total proportion of total marginal frequency of observations. Suitability category Kappa coefficient < 0 (less than chance agreement), 0.01–0.20 (slight agreement), 0.21–0.40 (fair agreement), 0.41–0.60 (moderate agreement), 0.61–0.80 (substantial agreement), and 0.81–0.99 (almost perfect agreement) (Viera & Garrett, 2005).

Image preprocessing Multiple processes were employed to ensure that the images in the collected Landsat datasets were suitable for analysis. We utilized the DOS (Dark-Object Subtraction) method, an atmospheric correction implemented during the image preparation phase (Niraj et al., 2022; Kakati et al., 2023). Followed by image channels merging (band combination). Preprocessing was done using QGIS 3.20 and the addition of the Semi-Automatic Classification Plugin (SCP), a robust open-source or free software, for land preparation tasks (Leroux et al., 2018; Alraey, 2022; Brel et al., 2022).

Vegetation indices The VIs are commonly employed to analyze vegetation dynamics at various scales by capturing information about photosynthetic activity and canopy structure using remote sensing (Zeng et al., 2022). The selection of the five VIs was based on their proven effectiveness in monitoring vegetation health and cover across various ecosystems. Each index has distinct characteristics that complement one another, providing a comprehensive assessment of agroforestry land cover in the Lampung Province. ARVI was chosen for its ability to reduce atmospheric effects, such as aerosols, which are particularly significant in regions like Lampung that may experience haze or pollution. EVI was included because of its sensitivity to canopy structure and ability to minimize soil background influences, making it particularly useful in densely vegetated areas. NDVI is a widely used index for detecting green vegetation. Its extensive use in literature and ease of application made it an essential choice for ensuring comparability with other studies. SAVI was selected to correct for the influence of soil brightness, making it particularly useful in areas with sparse vegetation or bare soil, which is common in parts of the study area GDVI focuses on the green band, which offers better sensitivity to vegetation in certain conditions compared to the red band used by NDVI. It is particularly effective in identifying healthy vegetation (Somvanshi & Kumari, 2020).

These VIs have been employed in several domains such as phenology, vegetation classification, photosynthetic activity, aboveground net primary productivity, and land surface temperature (Zhu et al., 2016; Langhe et al., 2020; Liu et al., 2020; Vorovencii, 2021).

In this study, several VIs have been simultaneously utilized in calculations to accurately identify agroforestry land, namely: atmospherically resistant vegetation index (ARVI), enhanced vegetation index (EVI), green difference vegetation index (GDVI), normalized difference vegetation index (NDVI), and soil-adjusted vegetation index (SAVI) (Table 2).

Vegetation indices assessment Descriptive statistics were used to assess the values of several VIs read at each POI. ANOVA was then performed to analyze the variance (p -value < 0.01). Tukey's test (p -value < 0.05) was used to complete the study and find the mean differences in the values of numerous VIs.

Decision tree DT is a hierarchical structure resembling a flow chart, with rectangular nodes representing internal decisions and oval nodes representing final outcomes. The land use classes were identified using a DT classifier, which utilized the five studied VIs. The DT was developed based on various levels of decision-making, taking into account the characteristics of the input datasets (Mountrakis et al., 2011). While DT has certain limitations, such as a tendency to overfit and sensitivity to small variations in the data, DT was chosen for this study due to its simplicity, interpretability, and efficiency in classification tasks (Czajkowski & Kretowski, 2019). The DT algorithm was widely utilized due to its simplicity of implementation and greater comprehensibility in comparison to other categorization algorithms (Yadav & Pal, 2012). The construction of a DT is rather rapid in comparison to alternative classification approaches (Anyanwu & Shiva, 2009). These qualities are particularly important in agroforestry land use and land cover (LULC) classification, where the ability to interpret and understand the decision-making process is crucial for informing land management policies and decisions. The DT algorithm allows for clear, straightforward rules to be derived from the data, which can be easily communicated to non-technical stakeholders, such as policymakers and land managers.

Results and Discussion

Land use types validations Land use types and accuracy testing involve verifying the validity of digital analysis outcomes by comparing producer accuracy derived from satellite imagery LULC processing with user's accuracy derived from ground truth data. An effective method to assess accuracy was by employing an error matrix or confusion matrix (Pahleviannur, 2019). The error matrix table was not only utilized to acquire the accuracy of all categories but also the accuracy of each category (Derajat et al., 2020). The United States Geological Survey (USGS) has established a minimal threshold for categorization or interpretation accuracy in remote sensing, specifically at 85%. (Wan et al., 2019; Shinskie et al., 2023).

Validation tests of land use types were based on POI in the field on 7 types of LULC. The calculation findings indicated that the producer accuracy for each category of LULC falls within the range of 88.64% to 93.66%, while the user accuracy calculation results vary from 87.75% to 94.75%. The overall accuracy calculation demonstrated a precision of 0.9158, or 91.58%, indicating a high level of accuracy (Table 3). This exceeds the minimum requirement specified by the USGS for land use analysis accuracy (Viera & Garrett, 2005; Sampurno & Thoriq, 2016; Cabrera et al., 2020; Congedo, 2021).

Likewise, the Kappa coefficient calculation yields lesser findings compared to the calculated results, specifically 0.9018 or 90.18%. The Kappa coefficient value satisfies the criteria to confirm that the chosen POI in the study can serve as a reliable reference for conducting additional analysis on the identification of agroforestry land use using image data for different VIs.

Characteristics of vegetation index The ARVI vegetation index ranged from -0.69 to 0.99, with a range of 1.68 while the EVI vegetation index ranged from -1.00 to 0.99, with a range of 1.99. The GDVI vegetation index ranged from -0.76 to 0.95, with a range of 1.71 while The NDVI vegetation index ranged from -1.00 to 0.99, with a range of 1.99. Regarding the SAVI vegetation index, the minimum value recorded was -0.72, while the maximum value was 0.92, resulting in a range of 1.64 (Table 4). The water body LULC type exhibited the lowest index value for overall VIs employed in this research, while the forest LULC type demonstrated the greatest for all VIs value detected (Figure 2).

Table 2 Technical description of the vegetation indices

Index	Fullname	Formula	References
ARVI	Atmospherically resistant vegetation index	$(\text{NIR Band} - (2 * \text{Red Band}) + \text{Blue Band}) / (\text{NIR} + (2 * \text{Red Band}) + \text{Blue Band})$	(Kaufman & Tanré, 1992)
EVI	Enhanced vegetation index	$2.5 * ((\text{NIR Band} - \text{Red Band}) / ((\text{NIR Band} + 6 * \text{Red Band} - 7.5 * \text{Blue Band}) + 1))$	(Huete, 1988)
GDVI	Green difference vegetation index	$\text{NIR Band} - \text{Green Band}$	(Wu, 2014)
NDVI	Normalized difference vegetation index	$(\text{NIR Band} - \text{Red Band}) / (\text{NIR Band} + \text{Red Band})$	(Rouse et al., 1973)
SAVI	Soil-adjusted vegetation index	$(1.5 * (\text{NIR Band} - \text{Red Band})) / ((\text{NIR Band} + \text{Red Band} + 0.5))$	(Huete, 1988)

Table 3 Point of interest confusion matrix in various LULC types

Land use types	X1	X2	X3	X4	X5	X6	X7	Total rows	User's accuracy (%)
Forest	8	0	2	7	1	41	741	800	92.63
Agroforestry	7	10	3	13	14	725	28	800	90.63
Dry land farming	5	35	10	5	725	18	2	800	90.63
Ricefield	21	19	0	734	18	8	0	800	91.75
Water Bodies	741	6	2	29	8	3	11	800	92.63
Settlements	17	12	751	4	12	3	1	800	93.88
Bare land	22	712	25	6	30	5	0	800	89.00
Total column	821	794	793	798	808	803	783	5,600	
Producer accuracy (%)	90.26	89.67	94.70	91.98	89.73	90.29	94.64		

Note: X1 = water body; X2 = bare land; X3 = settlements; X4 = ricefield; X5 = dry land farming; X6 = agroforestry; X7 = forest.

Table 4 Range of values for various vegetation indicestypes

Vegetatiton indices	Minimum	Maximum	Range
ARVI	-0.69	0.99	1.68
EVI	-1.00	0.99	1.99
GDVI	-0.76	0.95	1.71
NDVI	-1.00	0.99	1.99
SAVI	-0.72	0.92	1.64

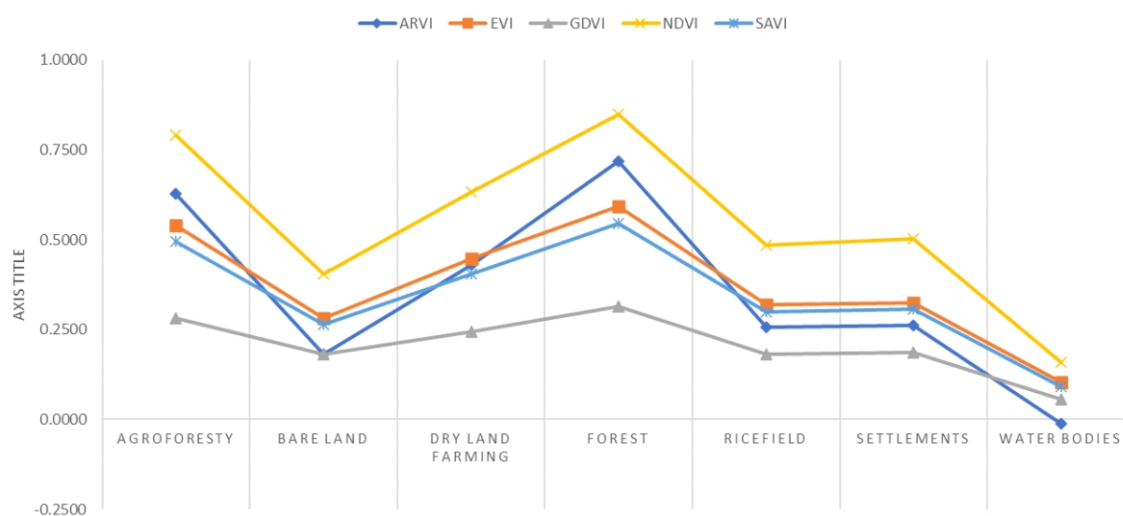


Figure 2 Distribution of vegetation index values.

The vegetation index values read at each POI were analyzed using ANOVA (p -value < 0.01) and followed by Tukey's advanced test (p -value < 0.05). The calculation results show that the average value of the vegetation index for various types of LULC was quite different, but there are several types of land use where the average value was not significantly different.

In the ARVI, NDVI, and SAVI, the types of LULC for settlements and rice fields are not significantly different. Meanwhile, in the EVI and GDVI, the types of LULC, cloud cover, settlements, and rice fields do not differ significantly. Details of the mean values and standard errors for each vegetation index for various types of LULC can be seen in Table 5.

Threshold vegetation index for agroforestry LULC The threshold calculation for the vegetation index for agroforestry LULC was carried out using DT, where the five VIs along with the index values read from 5,600 POIs in seven LULC classes for the 5 VIs were included in the calculation.

The DT used in this research was the QUEST (quick, unbiased, efficient statistical tree) model, which is a binary classification method that has advantages over classification models, especially in terms of the established genetic algorithm rules and the stochastic approach, which allows different outputs to be executed to achieve optimal results (Stockwell & Peters, 1999). In addition, QUEST is assessed as a DT model with fast, impartial, and efficient processing,

using a linear or unbiased variable selection model and using imputation (replacing missing data with estimates of input data variables with other alternatives) rather than replacement separation. (substitute splits) to handle missing data (Szufa et al., 2023).

The DT results for the agroforestry LULC type show that to classify the NDVI and ARVI in stages. Where areas with an NDVI index value > 0.6075 to $NDVI < 0.7756$ and an ARVI index value > 0.4842 are agroforestry LULC types. Various vegetation indices map for the Lampung Province region can be seen in Figure 3.

Table 5 Mean value and standard error of each vegetation index for various type of LULC

Vegetation indices	Land use types						
	X1	X2	X3	X4	X5	X6	X7
ARVI	-0.01 ± 0.01 a	0.18 ± 0.01 b	0.26 ± 0.00 c	0.26 ± 0.01 c	0.43 ± 0.01 d	0.63 ± 0.00 e	0.72 ± 0.00 f
EVI	0.10 ± 0.01 a	0.28 ± 0.01 b	0.32 ± 0.00 c	0.32 ± 0.01 c	0.45 ± 0.00 d	0.54 ± 0.00 e	0.59 ± 0.00 f
GDVI	0.06 ± 0.00 a	0.18 ± 0.00 b	0.19 ± 0.00 b	0.18 ± 0.00 b	0.24 ± 0.00 c	0.28 ± 0.00 d	0.31 ± 0.00 e
NDVI	0.16 ± 0.01 a	0.40 ± 0.01 b	0.50 ± 0.00 c	0.49 ± 0.01 c	0.63 ± 0.01 d	0.79 ± 0.00 e	0.85 ± 0.00 f
SAVI	0.09 ± 0.01 a	0.26 ± 0.00 b	0.31 ± 0.00 c	0.30 ± 0.00 c	0.41 ± 0.00 d	0.50 ± 0.00 e	0.55 ± 0.00 f

Note: X1 = water body; X2 = bare land; X3 = settlements; X4 = ricefield; X5 = dry land farming; X6 = agroforestry; X7 = forest.

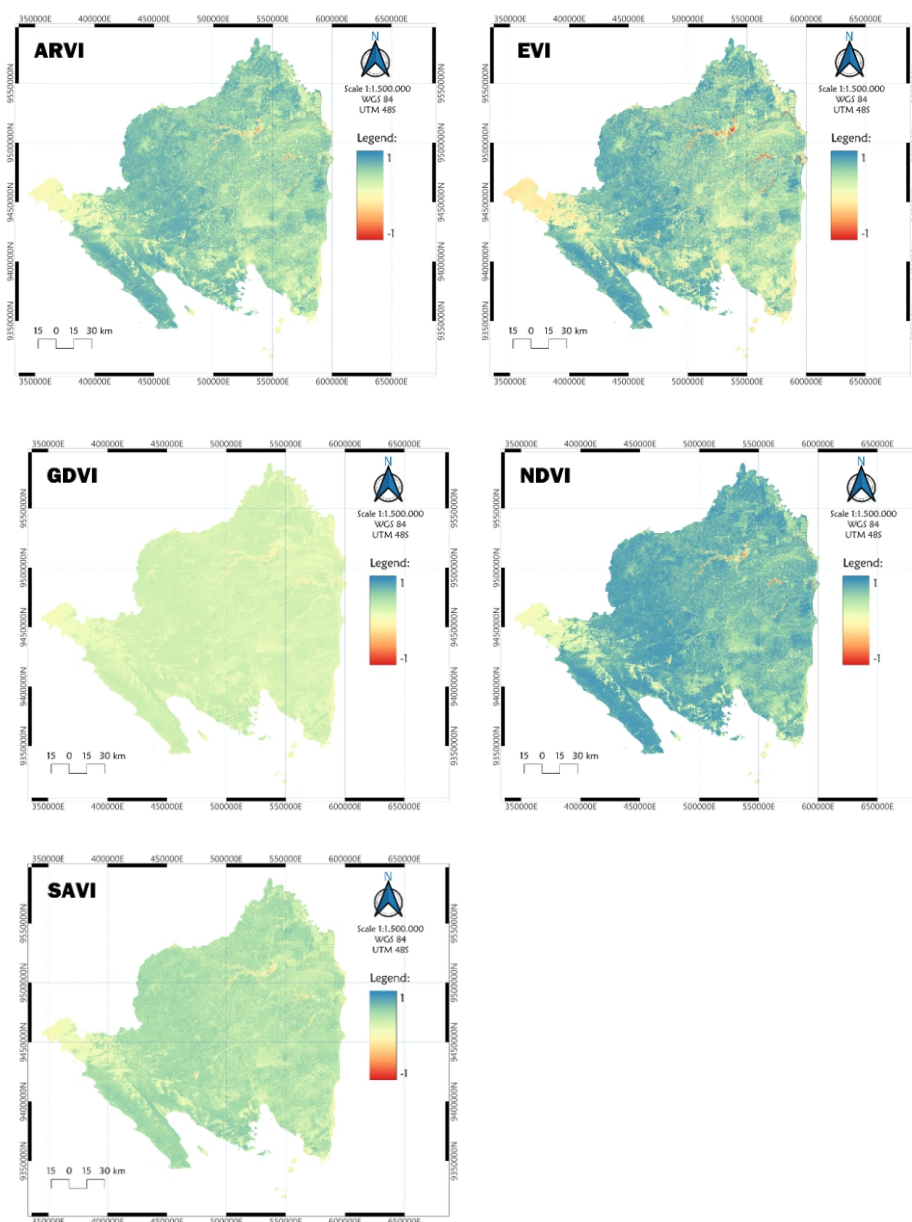


Figure 3 Various vegetation indices for the Lampung Province region.

Estimated area of agroforestry in Lampung Province

Estimating the area of agroforestry LULC in Lampung Province was conducted using DT. The result from DT classification showed that only ARVI and NDVI had the greater refinement in identifying agroforestry areas by leveraging the sensitivity of these indices to vegetation greenness and canopy density (Figure 4). This approach ensured that the classification process took into account the nuanced differences between agroforestry and other land cover types, providing more accurate results.

Separation of agroforestry LULC types in the ARVI and NDVI vegetation index raster images begins with the geospatial operation "Reclassify by Table" or reclassification, which functions to change the digital number values in the raster image into categories and class labels (Lacaze et al., 2018; Passy & Théry 2018; Camacho Olmedo & García-Álvarez, 2022).

The next step is to convert the reclassified image into a vector using the geospatial operation "Polygonize", where this operation has the function of changing raster format to

vector (Vitalis et al., 2020; Song et al., 2023).

Following the polygonization and formation of vector data, the "Extract by Attribute" operation is utilized to extract an area containing only agroforestry LULC. The value chosen for this operation corresponds to the class category, specifically the class 2 category, which represents the agroforestry LULC area (Table 6).

The final results of the area of agroforestry land cover in all areas of Lampung Province show that the estimated area of agroforestry reached 734,739.61 ha. The extent and distribution of agroforestry areas in Lampung Province can be seen in Figure 5. Using the intersection operation on agroforestry LULC areas on the ARVI and NDVI indices resulted from the DT algorithm. The following step was to obtain intersecting functions to list all intersection vectors between geographic area polygons and agroforestry area distribution polygons (Packert et al., 2020; Widaningrum, 2022). Finally, the geometry calculator was used to calculate the agroforestry area. The overall estimation indicated that the agroforestry area in Lampung Province spans 734,739.61 ha.

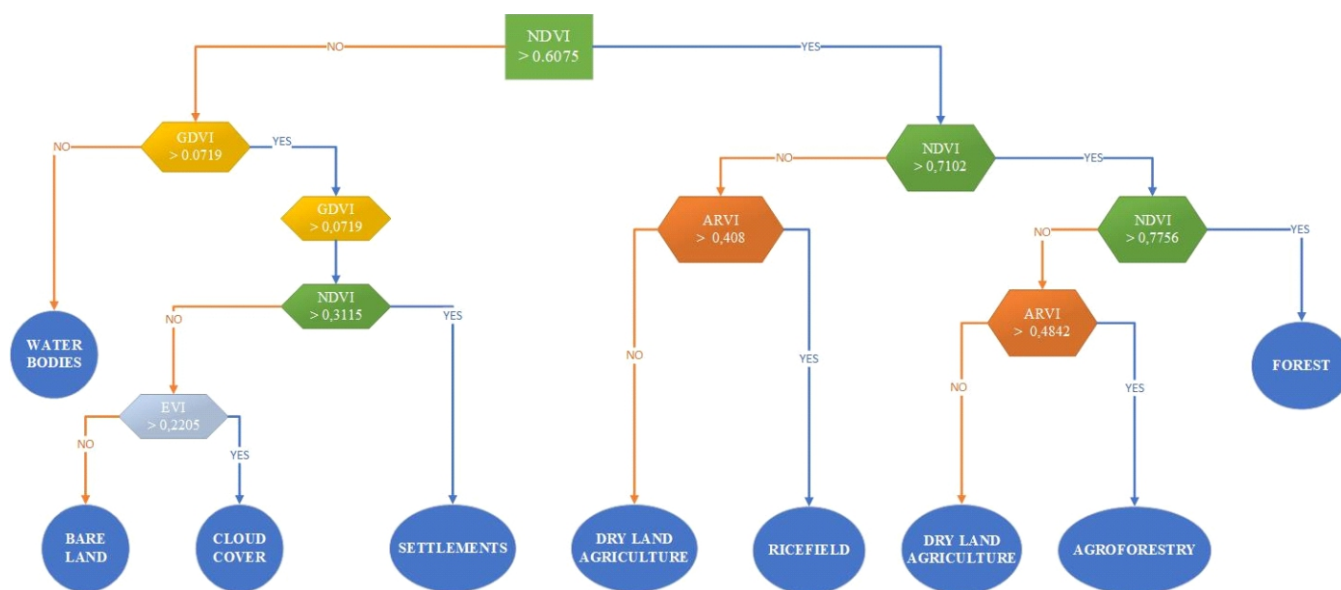


Figure 4 Decision tree land use land change class results with 5 vegetation indices.

Table 6 Mean value and standard error of each vegetation index for various type of LULC

Vegetation indices	Index value	LULC types
ARVI	≤ 0.4667	Non agroforestry
	> 0.4667	Agroforestry
NDVI	≤ 0.6074	Non agroforestry
	$> 0.6074 - \leq 0.7512$	Agroforestry
	> 0.7512	Non agroforestry

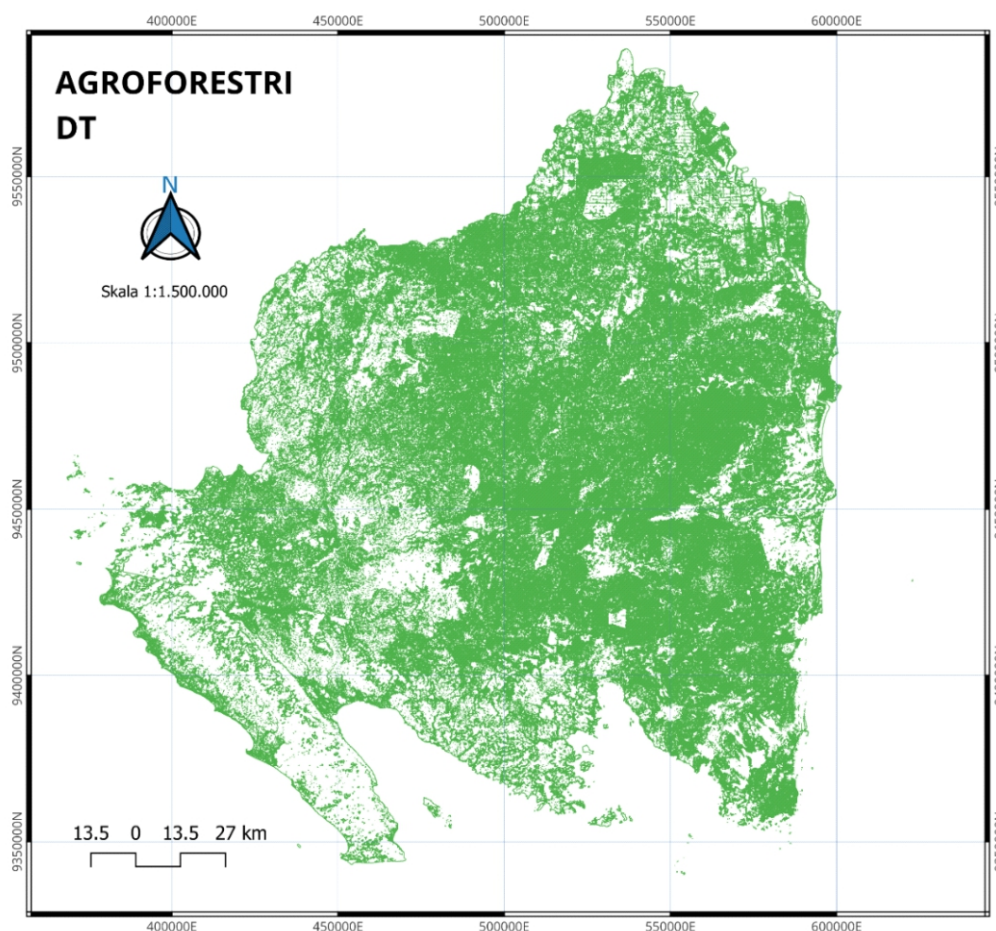


Figure 5 Agroforestry land use land change resulted from decision tree algorithm.

Conclusion

Each vegetation index was assigned its own specific threshold value based on the characteristics of the land cover types, ensuring a more accurate classification of agroforestry areas. The identification and segregation of distinct agroforestry areas included the use of just ARVI and NDVI. Both vegetation indices were chosen through DT algorithm processing. The estimated agroforestry area of 734,739.61 ha was derived. The study emphasizes the effectiveness of DT based on various VIs techniques in accurately assessing agroforestry in Lampung Province. The application of advanced techniques such as DTs for establishing thresholds and geospatial operations for estimating areas enhances the reliability of the outcomes. The findings provide valuable insights for land management and ecological planning in the Lampung Province region.

Acknowledgment

The authors would like to thank the support of various parties who helped carry out this research. We also would like to thank the University of Lampung for the funds allocated for this research through the “*Penelitian Terapan*” grant scheme with contract number 758/UN26.21/PN/2023.

References

Afifah, F. A. N., Febryano, I. G., Santoso, T., & Darmawan,

A. (2021). Identifikasi perubahan penggunaan lahan agroforestri di Pulau Pahawang. *Journal of Tropical Marine Science*, 4(1), 1–8. <https://doi.org/10.33019/jour.trop.mar.sci.v4i1.2037>

Akmal, R. R., Winarno, G. D., & Santoso, T. (2021). Pemetaan jalur interpretasi ekowisata di Desa Pahungan, Kabupaten Pesisir Barat. *Jurnal Hutan Tropis*, 9(1), 173–180. <https://doi.org/10.20527/jht.v9i1.10492>

Alhabsyi, T., Bempah, I., & Tolinggi, W. K. (2020). Analisis implementasi kebijakan pemerintah daerah terhadap penggunaan lahan sistem agroforestri di Kecamatan Suwawa Selatan Kabupaten Bone Bolango. *AGRINESIA: Jurnal Ilmiah Agribisnis* 4(2), 118–126. <https://doi.org/10.37046/agr.v4i2.9778>

Alraey, Y. (2022). Distribution and epidemiological features of cutaneous leishmaniasis in Asir Province, Saudi Arabia, from 2011 to 2020. *Journal of Infection and Public Health*, 15(7), 757–765. <https://doi.org/10.1016/j.jiph.2022.05.015>

Anyanwu, M. N., & Shiva, S. G. (2009). Comparative analysis of serial decision tree classification algorithms. *International Journal of Computer Science and Security*, 3(3), 230–240.

- Ardiansyah, M., Nugroho, B., & Al-Fajar, A. (2022). Respon spektral tajuk jagung pada beberapa perlakuan pemupukan. *Jurnal Ilmu Tanah dan Lingkungan*, 24(1), 25–31. <https://doi.org/10.29244/jitl.24.1.25-31>
- Aryal, D. R., Corzo, R. R., Cruz, A. L., Sanabria, C. V., Castro, H. G., Hernández, F. G., Ruiz, R. P., Venegas, J. A. V., Coss, A. L. de, Ruiz, D. M., & Chi, I. E. (2018). Biomass accumulation in forests with high pressure of fuelwood extraction in Chiapas, Mexico. *Revista Arvore*, 42(3), e420307. <https://doi.org/10.1590/1806-90882018000300007>
- Benharrats, F., & Mahi, H. (2020). Surface solar radiation modeling from Landsat 8 OLI/TIRS satellite data. *2020 5th International Conference on Renewable Energies for Developing Countries (REDEC)*. <https://doi.org/10.1109/REDEC49234.2020.9163851>
- Berhane, T. M., Lane, C. R., Wu, Q., Autrey, B. C., Anenkhonov, O. A., Chepinoga, V. V., & Liu, H. (2018). Decision-tree, rule-based, and random forest classification of high-resolution multispectral imagery for wetland mapping and inventory. *Remote Sensing*, 10(4), 580. <https://doi.org/10.3390/rs10040580>
- Binte Mostafiz, R., Noguchi, R., & Ahamed, T. (2021). Agricultural land suitability assessment using satellite remote sensing-derived soil-vegetation indices. *Land*, 10(2), 223. <https://doi.org/10.3390/land10020223>
- [BPS] Badan Pusat Statistik Provinsi Lampung. (2023). *Lampung dalam angka 2023*. Bandar Lampung: BPS Lampung.
- Brel, O. A., Zaytseva, A. I., Kaizer, P. J., & Migal, A. S. (2022). Spatial organization of industrial tourism objects: Case of the Kemerovo Region-Kuzbass. *Geo Journal of Tourism and Geosites*, 44(4), 1306–1311. <https://doi.org/10.30892/gtg.44415-947>
- Cabrera, E., Galindo, G., González, J., Vergara, L., Forero, C., Cubillos, A., Espejo, J., Rubiano, J., Corredor, X., Hurtado, L., Vargas, D., & Duque, A. (2020). Colombian forest monitoring system: Assessing deforestation in an environmental complex country. *Forest Degradation Around the World*. IntechOpen. <https://doi.org/10.5772/intechopen.86143>
- Camacho Olmedo, M. T., & García-Álvarez, D. (2022). Basic and multiple-resolution cross-tabulation to validate land use cover maps. In D. García-Álvarez, M. T. Camacho Olmedo, M. Paegelow, & J. F. Mas (Eds.), *Land use cover datasets and validation tools* (pp. 99–125). Springer. https://doi.org/10.1007/978-3-030-90998-7_7
- Congedo, L. (2021). Semi-automatic classification plugin: A python tool for the download and processing of remote sensing images in QGIS. *Journal of Open Source Software* 6(64), 3172. <https://doi.org/10.21105/joss.03172>
- Czajkowski, M., & Kretowski, M. (2019). Decision tree underfitting in mining of gene expression data. An evolutionary multi-test tree approach. *Expert Systems with Applications*, 137, 392–404. <https://doi.org/10.1016/j.eswa.2019.07.019>
- Damayanti, D. R., Bintoro, A., & Santoso, T. (2017). Permudaan alami hutan di satuan pengelolaan Taman Nasional (SPTN) Wilayah III Kuala Penet Taman Nasional Way Kambas. *Jurnal Sylva Lestari*, 5(1), 92–104.
- Derajat, R. M., Sopariah, Y., Aprilianti, S., Candra Taruna, A., Rahmawan Tisna, H. A., Ridwana, R., & Sugandi, D. (2020). Klasifikasi tutupan lahan menggunakan citra Landsat 8 Operational Land Imager (OLI) di Kecamatan Pangandaran. *Jurnal Samudra Geografi*, 3(1), 1–10. <https://doi.org/10.33059/jsg.v3i1.1985>
- Dogru, A. O., Goksel, C., David, R. M., Tolunay, D., Sözen, S., & Orhon, D. (2020). Detrimental environmental impact of large scale land use through deforestation and deterioration of carbon balance in Istanbul Northern Forest Area. *Environmental Earth Sciences*, 79(11), 270. <https://doi.org/10.1007/s12665-020-08996-3>
- Gama-Rodrigues, A. C., Müller, M. W., Gama-Rodrigues, E. F., & Mendes, F. A. T. (2021). Cacao-based agroforestry systems in the Atlantic Forest and Amazon Biomes: An ecoregional analysis of land use. *Agricultural Systems*, 194, 103270. <https://doi.org/10.1016/j.agsy.2021.103270>
- Gao, Y., Liu, L., Zhang, X., Chen, X., Mi, J., & Xie, S. (2020). Consistency analysis and accuracy assessment of three global 30-m land-cover products over the European Union using the lucas dataset. *Remote Sensing*, 12(21), 3479. <https://doi.org/10.3390/rs12213479>
- Gosling, E., Reith, E., Knoke, T., Gerique, A., & Paul, C. (2020). Exploring farmer perceptions of agroforestry via multi-objective optimisation: A test application in Eastern Panama. *Agroforestry Systems*, 94(5), 2003–2020. <https://doi.org/10.1007/s10457-020-00519-0>
- Guerini Filho, M., Kuplich, T. M., & Quadros, F. L. F. D. (2020). Estimating natural grassland biomass by vegetation indices using Sentinel 2 remote sensing data. *International Journal of Remote Sensing*, 41(8), 2861–2876. <https://doi.org/10.1080/01431161.2019.1697004>
- Hariato, S. P., Surnayanti, S., Tsani, M. K., & Santoso, T. (2022). Utilizing market waste to create organic waste in Teluk Pandan, Pesawaran. *Community Empowerment* 7(11), 1873–1880. <https://doi.org/10.31603/ce.7815>
- Hidayati, I. N., Suharyadi, R., & Danoedoro, P. (2019). Exploring spectral index band and vegetation indices for estimating vegetation area. *Indonesian Journal of Geography*, 50(2), 211–221. <https://doi.org/10.22146/ijg.38981>

- Huang, H. G., & Lian, J. (2015). A 3D approach to reconstruct continuous optical images using lidar and modis. *Forest Ecosystems*, 2(1), 20. <https://doi.org/10.1186/s40663-015-0044-5>
- Huang, S., Tang, L., Hupy, J. P., Wang, Y., & Shao, G. (2021). Correction to: Commentary review on the use of normalized difference vegetation index (NDVI) in the era of popular remote sensing. *Journal of Forestry Research*, 32, 2719. <https://doi.org/10.1007/s11676-020-01176-w>
- Huete, A. R. 1988. A soil-adjusted vegetation index (SAVI). *Remote sensing of environment*, 25(3), 295–309. [https://doi.org/10.1016/0034-4257\(88\)90106-X](https://doi.org/10.1016/0034-4257(88)90106-X)
- Jaya, I. N. S., & Etyarsah, S. (2021). *Analisis citra digital perspektif penginderaan jauh untuk pengelolaan sumber daya alam*. Bogor: IPB Press.
- Jezeer, R. E., Santos, M. J., Verweij, P. A., Boot, R. G. A., & Clough, Y. (2019). Benefits for multiple ecosystem services in Peruvian coffee agroforestry systems without reducing yield. *Ecosystem Services*, 40, 101033. <https://doi.org/10.1016/j.ecoser.2019.101033>
- Jorge, J., Vallbé, M., & Soler, J. A. (2019). Detection of irrigation inhomogeneities in an olive grove using the NDRE vegetation index obtained from UAV images. *European Journal of Remote Sensing*, 52(1), 169–177. <https://doi.org/10.1080/22797254.2019.1572459>
- Kakati, R., Dwivedy, S. K., & Dutta, S. (2023). Development of a fully automated atmospheric correction technique for applications in Google Earth Engine. In S. Dutta, & V. Chembolu (Eds.), *Recent development in river corridor management. RCRM 2022. Lecture notes in civil engineering* (pp. 337–348). Springer. https://doi.org/10.1007/978-981-99-4423-1_24
- Kaufman, Y. J., & Tanré, D. (1992). Atmospherically resistant vegetation index (ARVI) for EOS-MODIS. *IEEE Transactions on Geoscience and Remote Sensing*, 30(2), 261–270. <https://doi.org/10.1109/36.134076>
- Lacaze, B., Dudek, J., & Picard, J. (2018). GRASS GIS Software with QGIS. *QGIS and Generic Tools*, 1, 67–106. <https://doi.org/10.1002/9781119457091.ch3>
- Langhe, S., Herbei, M. V., & Sala, F. (2020). Use of remote sensing images in crop monitoring. Case study soybean crop. *Research Journal of Agricultural Science*, 52(4), 53–61.
- Leroux, L., Congedo, L., Bellón, B., Gaetano, R., & Bégué, A. (2018). Land cover mapping using Sentinel-2 images and the semi-automatic classification plugin: A Northern Burkina Faso Case Study. *QGIS and Applications in Agriculture and Forest*, 2, 119–151. <https://doi.org/10.1002/9781119457107.ch4>
- Li, X., Hu, T., Gong, P., Du, S., Chen, B., Li, X., & Dai, Q. (2021). Mapping essential urban land use categories in Beijing with a fast area of interest (AOI)-based method. *Remote Sensing*, 13(3), 477. <https://doi.org/10.3390/rs13030477>
- Liu, J., Zhang, J., Zhang, D., Jiao, S., Xing, J., Tang, H., Zhang, Y., Li, S., Zhou, Z., & Zuo, J. (2020). Sub-ambient radiative cooling with wind cover. *Renewable and Sustainable Energy Reviews*, 130, 109935. <https://doi.org/10.1016/j.rser.2020.109935>
- Logsdon, M. G., Bell, E. J., & Westerlund, F. V. (1996). Probability mapping of land use change: A GIS interface for visualizing transition probabilities. *Computers, Environment and Urban Systems*, 20(6), 389–398. [https://doi.org/10.1016/S0198-9715\(97\)00004-5](https://doi.org/10.1016/S0198-9715(97)00004-5)
- Maponya, P., Madakadze, C., Mbili, N., Dube, Z., Nkuna, T., Makhwedzhana, M., Tahulela, T., & Mongwaketsi, K. (2021). Potential constraint of rainfall availability on the establishment and expansion of agroforestry in the Mopani District, Limpopo Province in South Africa. *Agrofor*, 6(1), 26–35. <https://doi.org/10.7251/agreng2101026m>
- Markham, B. L., Jenstrom, D., Masek, J. G., Dabney, P., Pedelty, J. A., Barsi, J. A., & Montanaro, M. (2016). Landsat 9: Status and plans. *Proceedings Society of Photo-Optical Instrumentation Engineers 9972, Earth Observing Systems XXI*, 99720G. <https://doi.org/10.1117/12.2238658>
- Masek, J. G., Wulder, M. A., Markham, B., McCorkel, J., Crawford, C. J., Storey, J., & Jenstrom, D. T. (2020). Landsat 9: Empowering open science and applications through continuity. *Remote Sensing of Environment*, 248, 111968. <https://doi.org/10.1016/j.rse.2020.111968>
- Maxwell, A. E., Warner, T. A., & Guillén, L. A. (2021). Accuracy assessment in convolutional neural network-based deep learning remote sensing studies part 2: Recommendations and best practices. *Remote Sensing*, 13(13), 2450. <https://doi.org/10.3390/rs13132591>
- Miller, G. J., Morris, J. T., & Wang, C. (2019). Estimating aboveground biomass and its spatial distribution in coastal wetlands utilizing planet multispectral imagery. *Remote Sensing*, 11(17), 2020. <https://doi.org/10.3390/rs11172020>
- [MoEF] Minister of Environment and Forestry. (2021). *Peraturan Menteri Lingkungan Hidup dan Kehutanan Nomor 27 Tahun 2021 tentang Indeks Kualitas Lingkungan Hidup*. Jakarta: Minister of Environment and Forestry.
- Mishra, V. N., Kumar, V., Prasad, R., & Punia, M. (2021). Geographically weighted method integrated with logistic regression for analyzing spatially varying accuracy measures of remote sensing image classification. *Journal of the Indian Society of Remote Sensing*, 49(5), 1189–1199. <https://doi.org/10.1007/s12524-020-01286-2>
- Mountrakis, G., Im, J., & Ogole, C. (2011). Support vector

- machines in remote sensing: A review. *ISPRS Journal of Photogrammetry and Remote Sensing*, 66(3), 247–259. <https://doi.org/10.1016/j.isprsjprs.2010.11.001>
- Musiaka, Ł., & Nalej, M. (2021). Application of GIS tools in the measurement analysis of urban spatial layouts using the square grid method. *ISPRS International Journal of Geo-Information*, 10(8), 558. <https://doi.org/10.3390/ijgi10080558>
- Narendra, B. H., Siregar, C. A., Turjaman, M., Hidayat, A., Rachmat, H. H., Mulyanto, B., Maharani, R., Rayadin, Y., Prayudyaningsih, R., & Yuwati, T. W. (2021). Managing and reforesting degraded post-mining landscape in Indonesia: A review. *Land*, 10(6), 658. <https://doi.org/10.3390/land10060658>
- Niraj, K. C., Gupta, S. K., & Shukla, D. P. (2022). A comparison of image-based and physics-based atmospheric correction methods for extracting snow and vegetation cover in Nepal Himalayas using Landsat 8 OLI images. *Journal of the Indian Society of Remote Sensing*, 50(12), 2503–2521. <https://doi.org/10.1007/s12524-022-01616-6>
- Octavia, D., Suharti, S., Murniati, Dharmawan, I. W. S., Nugroho, H. Y. S. H., Supriyanto, B., Rohadi, D., Njurumana, G. N., Yeny, I., Hani, A., Mindawati, N., Suratman, Adalina, Y., Prameswari, D., Hadi, E. E. W., & Ekawati, S. (2022). Mainstreaming smart agroforestry for social forestry implementation to support sustainable development goals in Indonesia: A review. *Sustainability*, 14(15), 9313. <https://doi.org/10.3390/su14159313>
- Oon, A., Mohd Shafri, H. Z., Lechner, A. M., & Azhar, B. (2019). Discriminating between large-scale oil palm plantations and smallholdings on tropical peatlands using vegetation indices and supervised classification of Landsat-8. *International Journal of Remote Sensing*, 40(19), 7312–7328. <https://doi.org/10.1080/01431161.2019.1579944>
- Pahleviannur, M. R. (2019). Pemanfaatan informasi geospasial melalui interpretasi citra digital penginderaan jauh untuk monitoring perubahan penggunaan lahan. *JPIG (Jurnal Pendidikan dan Ilmu Geografi)*, 4(2), 18–26. <https://doi.org/10.21067/jpig.v4i2.3267>
- Passy, P., & Théry, S. (2018). The use of SAGA GIS Modules in QGIS. *QGIS and Generic Tools*, 1, 107–149. <https://doi.org/10.1002/9781119457091.ch4>
- Pôças, I., Calera, A., Campos, I., & Cunha, M. (2020). Remote sensing for estimating and mapping single and basal crop coefficients: A review on spectral vegetation indices approaches. *Agricultural Water Management*, 233, 106081. <https://doi.org/10.1016/j.agwat.2020.106081>
- Prasetya, A. Y., Qurniati, R., & Herwanti, S. (2020). Saluran dan margin pemasaran durian hasil agroforestri di Desa Sidodadi. *Jurnal Belantara*, 3(1), 32. <https://doi.org/10.29303/jbl.v3i1.315>
- Rahma, I. Y. (2020). Analisis komparasi metode pemetaan ekosistem mangrove menggunakan penginderaan jauh dan sistem informasi geografis. *Jurnal Geografi : Media Informasi Pengembangan dan Profesi Kegeografian*, 17(2), 49–55. <https://doi.org/10.15294/jg.v17i2.24417>
- Romli, K., Oktaviannur, M., Rinova, D., & Dharmawan, Y. Y. (2019). Analysis of tourism mapping in Lampung Province to optimize entrepreneurship development. *Review of Integrative Business and Economics Research*, 8, 110–118.
- Rouse, J. W. jr, Haas, R. H., Deering, D. W., Schell, J. A., & Harlan, J. C. (1973). *Monitoring the vernal advancement and retrogradation (green wave effect) of natural vegetation*. Progress Report RSC 1978-2. Texas A&M University Remote Sensing Center.
- Roy, B. (2021). Optimum machine learning algorithm selection for forecasting vegetation indices: MODIS NDVI & EVI. *Remote Sensing Applications: Society and Environment*, 23, 100582. <https://doi.org/10.1016/j.rsase.2021.100582>
- Rwanga, S. S., & Ndambuki, J. M. (2017). Accuracy assessment of land use/land cover classification using remote sensing and GIS. *International Journal of Geosciences*, 8(4), 611–622. <https://doi.org/10.4236/ijg.2017.84033>
- Sampurno, R., & Thoriq, A. (2016). Klasifikasi tutupan lahan menggunakan citra Landsat 8 Operational Land Imager (OLI) di Kabupaten Sumedang. *Jurnal Teknotan*, 10(2), 61–70. <https://doi.org/10.24198/jt.vol10n2.9>
- Santoso, T., Kartika, M., Surnayati, S., & Riniarti, M. (2021). Penggunaan citra DEMNAS untuk desain pola tanam alley cropping pada lahan garapan anggota KPPH Talang Mulya Kabupaten Pesawaran Provinsi Lampung. *ULIN: Jurnal Hutan Tropis*, 5(1), 33–40. <https://doi.org/10.32522/ujht.v5i1.4390>
- Santoso, T., Paridduar, R., & Bintoro, A. (2023). Plant diversity under traditional agroforestry system of repong damar in Pesisir Barat District, Lampung Province, Indonesia. *Biodiversitas*, 24(8), 4675–4684. <https://doi.org/10.13057/biodiv/d240849>
- Sari, R., Trihardianingsih, L., Mulya, R. F., Arief, M. I., & Kusri, K. (2022). Analisis index vegetation wilayah terdampak kebakaran hutan Riau menggunakan citra Landsat-8 dan Sentinel-2. *Cogito Smart Journal*, 8(2), 282–294. <https://doi.org/10.31154/cogito.v8i2.439.282-294>
- Saufi, S., & Saleh, M. (2021). Analisis karakteristik masyarakat agroforestri tanaman sengon di hutan produksi wilayah KPH Cantung. *JIEP: Jurnal Ilmu Ekonomi dan Pembangunan*, 4(2), 476–485. <https://doi.org/10.20527/jiep.v4i2.4404>
- Setiawan, K. T., Winarso, G., Ginting, D. N. B., Manessa, M., Anggraini, N., Hartuti, M., Asriningrum, W., &

- Parwati, E. (2021). Pemanfaatan metode semi-analitik untuk penentuan batimetri menggunakan citra satelit resolusi tinggi. *Jurnal Penginderaan Jauh dan Pengolahan Data Citra Digital*, 18(1), 1–13. <https://doi.org/10.30536/j.pjpdcd.2021.v18.a3409>.
- Setiawan, Y., Yoshino, K., & Philpot, W. D. (2013). Characterizing temporal vegetation dynamics of land use in regional scale of Java Island, Indonesia. *Journal of Land Use Science*, 8(1), 1–30. <https://doi.org/10.1080/1747423X.2011.605178>
- Shinskie, J. L., Delahunty, T., & Pitt, A. L. (2023). Fine-scale accuracy assessment of the 2016 National Land Cover Dataset for stream-based wildlife habitat. *The Journal of Wildlife Management*, 87(5), e22402. <https://doi.org/10.1002/jwmg.22402>
- Shishir, S., & Tsuyuzaki, S. (2018). Hierarchical classification of land use types using multiple vegetation indices to measure the effects of urbanization. *Environmental Monitoring and Assessment*, 190, 342. <https://doi.org/10.1007/s10661-018-6714-3>
- Sholihah, R. I., Trisasongko, B. H., Shiddiq, D., Iman, L. O. S., Kusdaryanto, S., Manijo, & Panuju, D. R. (2016). Identification of agricultural drought extent based on vegetation health indices of Landsat data: Case of Subang and Karawang, Indonesia. *Procedia Environmental Sciences*, 33, 14–20. <https://doi.org/10.1016/j.proenv.2016.03.051>
- Somvanshi, S. S., & Kumari, M. (2020). Comparative analysis of different vegetation indices with respect to atmospheric particulate pollution using sentinel data. *Applied Computing and Geosciences*, 7, 100032. <https://doi.org/10.1016/j.acags.2020.100032>
- Song, N., Sun, Q., Xu, S., Shan, D., Tang, Y., Tian, X., Xu, N., & Gao, J. (2023). Ultrawide-band optically transparent antidiffraction metamaterial absorber with a Thiessen-polygon metal-mesh shielding layer. *Photonics Research*, 11(7), 1354. <https://doi.org/10.1364/prj.486613>
- Stockwell, D., & Peters, D. (1999). The GARP modelling system: Problems and solutions to automated spatial prediction. *International Journal of Geographical Information Science*, 13(2), 143–158. <https://doi.org/10.1080/136588199241391>
- Szufa, S., Piersa, P., Junga, R., Błaszczuk, A., Modliński, N., Sobek, S., Marczak-Grzesik, M., Adrian, Ł., & Dzikuć, M. (2023). Numerical modeling of the co-firing process of an in situ steam-torrefied biomass with coal in a 230 MW industrial-scale boiler. *Energy*, 263, 125918. <https://doi.org/10.1016/j.energy.2022.125918>
- Tschora, H., & Cherubini, F. (2020). Co-benefits and trade-offs of agroforestry for climate change mitigation and other sustainability goals in West Africa. *Global Ecology and Conservation*, 22, e00919. <https://doi.org/10.1016/j.gecco.2020.e00919>.
- Tsendbazar, N., Herold, M., Li, L., Tarko, A., de Bruin, S., Masiliunas, D., Lesiv, M., Fritz, S., Buchhorn, M., Smets, B., van De Kerchove, R., & Duerauer, M. (2021). Towards operational validation of annual global land cover maps. *Remote Sensing of Environment*, 266, 112686. <https://doi.org/10.1016/j.rse.2021.112686>
- Viera, A. J., & Garrett, J. M. (2005). Understanding interobserver agreement: the Kappa statistic. *Family Medicine*, 37(5), 360–363.
- Visnhu, B. G. (2021). Diversifikasi olahan ubi kayu sebagai potensi Desa Sidomulyo dan penanaman ubi kayu dengan metode tumpang sari. *Jurnal Atma Inovasia*, 1(1), 8–13. <https://doi.org/10.24002/jai.v1i1.3905>
- Vitalis, S., Arroyo Ohori, K., & Stoter, J. (2020). CityJSON in QGIS: Development of an open-source plugin. *Transactions in GIS*, 24(5), 1147–1164. <https://doi.org/10.1111/tgis.12657>
- van Vliet, J., Bregt, A. K., Brown, D. G., van Delden, H., Heckbert, S., & Verburg, P. H. (2016). A review of current calibration and validation practices in land-change modeling. *Environmental Modelling and Software*, 82, 174–182. <https://doi.org/10.1016/j.envsoft.2016.04.017>
- Vorovencii, I. (2021). Changes detected in the extent of surface mining and reclamation using multitemporal Landsat imagery: a case study of Jiu Valley, Romania. *Environmental Monitoring and Assessment*, 193, 30. <https://doi.org/10.1007/s10661-020-08834-w>
- Wan, H., Shao, Y., Campbell, J. B., & Deng, X. (2019). Mapping annual urban change using time series Landsat and NLCD. *Photogrammetric Engineering & Remote Sensing*, 85(10), 715–724. <https://doi.org/10.14358/PERS.85.10.715>
- Wanderi, W., Qurniati, R., & Kaskoyo, H. (2019). Kontribusi tanaman agroforestri terhadap pendapatan dan kesejahteraan petani. *Jurnal Sylva Lestari*, 7(1), 118127. <https://doi.org/10.23960/jsl17118-127>
- Warren-Thomas, E., Nelson, L., Juthong, W., Bumrungsri, S., Brattström, O., Stroesser, L., Chambon, B., Penot, É., Tongkaemkaew, U., & Edwards, D. P. (2020). Rubber agroforestry in Thailand provides some biodiversity benefits without reducing yields. *Journal of Applied Ecology*, 57(1), 17–30. <https://doi.org/10.1111/1365-2664.13530>
- Wu, W. (2014). The generalized difference vegetation index (GDVI) for dryland characterization. *Remote Sensing*, 6(2), 1211–1233. <https://doi.org/10.3390/rs6021211>
- Wu, Z., Snyder, G., Vadnais, C., Arora, R., Babcock, M., Stensaas, G., Doucette, P., & Newman, T. (2019). User needs for future Landsat missions. *Remote Sensing of Environment*, 231, 111214. <https://doi.org/10.1016/j.rse.2019.111214>.

- Xie, F., & Fan, H. (2021). Deriving drought indices from MODIS vegetation indices (NDVI/EVI) and Land Surface Temperature (LST): Is data reconstruction necessary? *International Journal of Applied Earth Observation and Geoinformation*, 101, 102352. <https://doi.org/10.1016/j.jag.2021.102352>
- Xu, Y., Wang, L., Fu, C., & Kosmyna, T. (2017). A fishnet-constrained land use mix index derived from remotely sensed data. *Annals of GIS*, 23(4), 303–313. <https://doi.org/10.1080/19475683.2017.1382570>
- Yadav, S. K., & Pal, S. (2012). *Data mining: A prediction for performance improvement of engineering students using classification*. arXiv preprint arXiv:1203.3832. <https://doi.org/10.48550/arXiv.1203.3832>
- Zeng, Y., Hao, D., Huete, A., Dechant, B., Berry, J., Chen, J. M., Joiner, J., Frankenberg, C., Bond-Lamberty, B., Ryu, Y., Xiao, J., Asrar, G. R., & Chen, M. (2022). Optical vegetation indices for monitoring terrestrial ecosystems globally. *Nature Reviews Earth and Environment*, 3(7), 477–493. <https://doi.org/10.1038/s43017-022-00298-5>
- Zhao, H., Xu, L., Wang, Q., Tian, J., Tang, X., Tang, Z., Xie, Z., He, N., & Yu, G. (2018). Spatial patterns and environmental factors influencing leaf carbon content in the forests and shrublands of China. *Journal of Geographical Sciences*, 28(6), 791–801. <https://doi.org/10.1007/s11442-018-1505-x>
- Zhu, Z., Piao, S., Myneni, R. B., Huang, M., Zeng, Z., Canadell, J. G., Ciais, P., Sitch, S., Friedlingstein, P., Arneeth, A., Cao, C., Cheng, L., Kato, E., Koven, C., Li, Y., Lian, X., Liu, Y., Liu, R., Mao, J., ..., & Zeng, N. (2016). Greening of the earth and its drivers. *Nature Climate Change*, 6(8), 791–795. <https://doi.org/10.1038/nclimate3004>